


Cite this: *RSC Adv.*, 2018, 8, 35314

Growth inhibition of *Microcystic aeruginosa* by metal–organic frameworks: effect of variety, metal ion and organic ligand†

Gongduan Fan,^a  ^{ab} Liang Hong,^a Xiaomei Zheng,^a Jinjin Zhou,^a Jiajun Zhan,^a Zhong Chen^a and Siyuan Liu^a

Metal–organic frameworks (MOFs), as a new type of nanomaterial, have been rapidly developed and widely applied in the environmental area. However, the algae removal efficiency of MOFs, the effect of metal ions and organic ligands contained in MOFs and the stability of MOFs in water need further study. Based on the characteristics of algae, five types of MOFs, which were Cu-MOF-74, Zn-MOF-74, ZIF-8, Ag/AgCl@ZIF-8 and MIL-125(Ti) were synthesized and characterized by X-ray diffractometer (XRD), field emission scanning electron microscope (FESEM), and X-ray photoelectron spectroscopy (XPS). The effect of MOFs on the growth of *Microcystis aeruginosa* was comparatively studied, and the inhibition mechanism of MOFs on algae as well as the stability of MOFs was explored. Results showed that all of the as-synthetic MOFs had superior stability in water, and the order of stability of MOFs followed the order MIL-125(Ti) > Cu-MOF-74 > Ag/AgCl@ZIF-8 > ZIF-8 > Zn-MOF-74. The types of metal ions and organic ligands doped in MOFs have grade affected the inhibitory efficiency on the algae: containing Cu²⁺ and Ag⁺ ions, MOFs had more significant inhibitory capacity to algae than those containing Zn²⁺ ions; meanwhile, compared with MOFs which are assembled with 2,5-dihydroxyterephthalic acid (DHTA) organic ligands, MOFs containing 2-methylimidazole (GC) organic contributed to the removal of algae significantly. The order of inhibitory effects of algae by five MOFs follows the order Cu-MOF-74 > Ag/AgCl@ZIF-8 > ZIF-8 > Zn-MOF-74 > MIL-125(Ti). The physiological characteristics of algal cells were changed after being treated with different concentrations of Cu-MOF-74. Once the concentration of Cu-MOF-74 reached 1 mg L^{−1}, the algal cells began to be inhibited, the relative inhibition rate of algal cells at 120 h was over 400%, and the inhibition process fitted pseudo-second-order kinetic model well. The Cu²⁺ released by Cu-MOF-74 that the concentration higher than 1 mg L^{−1} would lead to the destruction of algae cell morphology and the loss of cell integrity, causing cell contents to be partially released into the water, promoting the accumulation and precipitation of algal cells which were destabilizing already to achieve the purpose of inhibition of algae. In summary, MOFs can be used to inhibit the growth of cyanobacteria and have a promising application prospect.

Received 1st July 2018
Accepted 23rd September 2018

DOI: 10.1039/c8ra05608k

rsc.li/rsc-advances

1 Introduction

In recent decades, harmful cyanobacteria blooms have frequently occurred in the eutrophic waters throughout the world.^{1–3} Cyanobacteria blooms have serious impacts on the quality of water environment, causing imbalance of aquatic ecosystems⁴ and endangering the safety of aquatic organisms and humans.^{5,6} Therefore, we urgently need an effective technique to remove cyanobacteria and control cyanobacteria

blooms. To control and eliminate harmful algal blooms, physical, chemical, and biological algae removal techniques, including ultrasonic method,⁷ reagent addition method,⁸ and biological interaction⁹ have been commonly applied. However, these conventional treatments suffer from drawbacks that limit their applicability such as relatively high cost, poor environmental acceptability, inefficiency of algae removal and so on. For example, the ultrasonic method has a high operating cost;¹⁰ direct addition of pesticides will cause adverse effects on organisms¹¹ as a result of secondary pollution;¹² and biological interaction has low algae removal efficiency.¹³ Therefore, it is still urgent to develop new remediation methods for the application of controlling cyanobacterial blooms, especially on the large-scale.

Nanomaterials have been widely used in the field of environmental modification and remediation for their advantages

^aCollege of Civil Engineering, Fuzhou University, 350116 Fujian, China. E-mail: fgdz@fzu.edu.cn^bDepartment of Chemical & Environmental Engineering, University of Arizona, 1133 E James E Rogers Way, Harshbarger 108, Tucson, AZ 85721-0011, USA

† Electronic supplementary information (ESI) available. See DOI: 10.1039/c8ra05608k



of high activity, low cost, and strong adsorption capacity.^{14,15} Nanomaterials can effectively inhibit the growth of algae cells, and their inhibition mechanism may include effects of metal ions,¹⁶ oxidative damage of ROS^{17,18} etc. Park *et al.*¹⁹ found that the inhibition efficiency of *Microcystis aeruginosa* (*M. aeruginosa*) was up to 87% when it was treated by 1 mg L⁻¹ nano-Ag. As a kind of porous nanocrystalline materials with periodic multidimensional network structure formed by self-assembly of metal ions and organic ligands such as aromatic polyacid through coordination, metal-organic frameworks (MOFs) have many advantages such as large surface area, high porosity, good thermal stability and easy to regulate physical and chemical properties.^{14,15} Their structure and properties give them great potential to be used in many fields such as catalysis, adsorption and environment.^{20,21} In the environmental area, MOFs have been proved to degrade organic dyes effectively in wastewater, Chandra *et al.*²² degraded rhodamine B and methylene blue in visible light using ZIF-8 loaded nano-TiO₂, and the removal rates of rhodamine B and methylene blue were 64.8%, and 87.5% respectively. In the catalysis field, MOFs have ability to remove drug residues from water bodies, Cao Yang *et al.*²³ used a MOF which was synthesized by MIL-68(In)-NH₂ and graphene oxide (GrO) for the photodegradation of amoxicillin, with the removal rate of 93%.

MOFs based on various metal ions such as Cu²⁺, Zn²⁺, Ag⁺ have different effects on the growth of algal cells.^{24,25} Furthermore, Keila Martin-Betancor *et al.*²⁶ found that the TAZ ligand in Ag-TAZ (50 mg L⁻¹) can cause 35% inhibition effect on *Anabaena*. The interactive effect between different ligands and metal ions, the effect on the morphology as well as the property of algae removal of MOFs due to the combination of different ligands with different metal ions were rarely studied, however, it is very important to select appropriate metal ions and ligands to synthesize corresponding MOFs according to the characteristics of algae to remove algae. In addition, Gu *et al.*²⁷ used Zn-Fe-LDHs (250 mg L⁻¹) as photocatalyst to inactivate the *M. aeruginosa* under visible light, the content of chlorophyll *a* decreased by 80.6%, which indicated the growth of *M. aeruginosa* was inhibited to some extent. However, this study only showed that the high concentration of MOFs material (Zn-Fe-LDHs) has inhibitory effect on algal cells, the impacts of MOFs material structure, metal ions and organic ligands on the inhibition of algae, the discipline between MOFs concentration and inhibition of algal, and the inhibition mechanism of algal cells by MOFs have not been further studied.

Therefore, according to the characteristics of algae, algae-sensitive metal ions such as Cu²⁺, Zn²⁺, Ag⁺ and organic ligands such as 2,5-dihydroxyterephthalic acid (DHTA), 2-methylimidazole (GC) and 1,4-dicarboxybenzene (PTA) were used to synthesize five MOFs materials including Cu-MOF-74, Zn-MOF-74, ZIF-8, Ag/AgCl@ZIF-8 and MIL-125(Ti). The physical properties of the five materials including composition and morphologies were characterized by x-radiation diffraction (XRD) and field emission scanning electron microscope (FESEM). The responses of the algae to prepared MOFs which were formed by the combination of different ions Cu²⁺, Zn²⁺, Ag⁺ and different organic ligands DHTA, GC and PTA were

studied. The discipline between the concentration of Cu-MOF-74 and the growth inhibition of algal cells, the effect of Cu-MOF-74 on the physiological characteristics of algal cells and the relevant inhibitive mechanism of algal by Cu-MOF-74 were explored, in expect to provide a theoretical basis for the application of MOFs in controlling and removing cyanobacterial cells in water.

2 Experiment and methods

2.1 Cyanobacteria inhibition experiment

2.1.1 Preparation of *M. aeruginosa* and MOFs stock solution. *M. aeruginosa* (FACHB 905, Chinese Academy of Sciences, China) were maintained in a liquid culture at 30 ± 1 °C using BG-11 growth medium (Blue-Green Medium). The initial pH of BG-11 medium²⁸ was adjusted to approximate 7.0.²⁹ The illumination was provided by a 2000 lx tubular fluorescent lamp, and companion with a 14 h : 10 h light-dark cycle. During the culture, the conical flask was shaken 3 times a day to ensure the normal growth of *M. aeruginosa* to the experimentally required growth capacity and absorbance.

MOFs, ligand and metal ions stock solution (1000 mg L⁻¹) was acquired by adding 0.01 g MOFs or ligand into 10 mL newly prepared BG-11 medium and underwent ultrasonic dispersion (40 kHz, 100 W) for 15 min.

2.1.2 Detection of OD₆₈₀ and growth inhibition rate in MOFs algae inhibition experiment. A blank control group was set without any treatment. The algal cells of the experimental groups were added with different volumes of MOFs stock solution to maintain the final concentration of MOFs in the algal cell suspension were 0.01, 0.05, 0.1, 1, 5, and 10 mg L⁻¹. All the algal cells including control group and experimental groups were cultivated companion with a 14 h : 10 h light-dark cycle by the illumination of 2000 lx tubular fluorescent lamp. The concentration of algal cells was measured using an UV-visible spectrophotometer (UV-Vis 2450, Shimadzu, Japan) with a wavelength of 680 nm at 2, 24, 48, 72, 96, and 120 h, respectively, since the optical density at 680 nm (OD₆₈₀) is linearly correlated with the algal cell concentration.

The growth inhibition rate of algal cells at different concentrations of MOFs was calculated by the inhibition rate formula (1) and (2) based on the specific growth rate:³⁰

$$\mu_{i-j} = \frac{\ln X_j - \ln X_i}{t_j - t_i} \quad (1)$$

$$I_r = \frac{\mu_C - \mu_T}{\mu_C} \times 100\% \quad (2)$$

where, μ_{i-j} is the specific growth rate from *i* h to *j* h; X_i and X_j are the OD₆₈₀ value at *i* h and *j* h respectively; I_r represents the inhibition rate based on the specific growth rate; μ_C is the average of the parallel specific growth rate of control group; μ_T is each parallel specific growth rate of experimental group.

2.1.3 Detection of Zeta potential in MOFs algae inhibition experiment. A blank control group was set and the algal cells in control group didn't undergo any treatment. The algal cells of the experimental groups were added with different volumes of



MOFs stock solution to maintain the final concentration of MOFs in the algal cell suspension were 0.01, 0.05, 0.1, 1, 5, and 10 mg L⁻¹. All the algal cells including control group and experimental groups were cultivated companion with a 14 h : 10 h light–dark cycle by the illumination of 2000 lx tubular fluorescent lamp. The Zeta potentials of algal cell solution in the control and different experimental groups were measured using a Zetasizer (Nano ZS90, Malvern, UK) at 2, 24, 48, 72, 96 and 120 h.

2.1.4 Detection of OD₆₈₀ in ligand inhibition algae cell experiment. A blank control group was set and the algal cells in control groups didn't do any treatment. The algal cells of the experimental groups were added with different volumes of ligands stock solution to maintain the final concentration of ligands in the algal cell suspension were 0, 1, 5, 10, 20, and 30 mg L⁻¹. All the algal cells including control groups and experimental groups were cultivated companion with a 14 h : 10 h light–dark cycle by the illumination of 2000 lx tubular fluorescent lamp. The concentration of algal cell was measured using an UV-visible spectrophotometer with a wavelength of 680 nm at 24, 48, 72, 96, and 120 h, respectively.

2.1.5 Detection of OD₆₈₀ in metal ions, P25 and Cu-MOF-74 inhibition algae cell experiment. A blank control group was set and the algal cells in control groups didn't do any treatment. The algal cells of the experimental groups were added with same volumes of P25, CuSO₄, AgNO₃ and Zn(NO₃)₂ stock solution to maintain the final concentration of metal ions and P25 in the algal cell suspension was 1 mg L⁻¹. All the algal cell including control groups and experimental groups were cultivated companion with a 14 h : 10 h light–dark cycle by the illumination of 2000 lx tubular fluorescent lamp. The concentration of algal cell was measured using an UV-visible spectrophotometer with a wavelength of 680 nm at 24, 48, 72, 96, and 120 h, respectively.

2.2 Cyanobacteria physiological characteristics experiment

2.2.1 Extracellular TOC detection of cyanobacteria. The algal cell suspension (16 mL) was centrifuged at 4500 rpm for 10 min with a centrifugal separator at room temperature. The collected supernatant was filtered through 0.45 μm filter, and then placed it in an autosampler to analyze the TOC value of algal cells by a total carbon analyzer (TOC-LCPH-CPN, Shimadzu, Japan).

2.2.2 Detection of cyanobacteria membrane integrity. The algal cell suspension (5 mL) was centrifuged at 5000 rpm for 10 min at room temperature. After that, discarding the supernatant and adding 1 mg L⁻¹ PI stock solution³¹ (1 mL), then incubated at room temperature in dark for 15–30 min. The cell membrane integrity of the algal cells was analyzed by flow cytometry (FACSCalibur, Beckman Coulter, USA) at the excitation wavelength of 488 nm, and the PI fluorescence for 10 000 cells was collected by the FL3 channel.

2.3 Cyanobacteria inhibition mechanism experiment

2.3.1 Detection of Cu²⁺ effects. The Cu-MOF-74 of 1 mg L⁻¹ stock solution was prepared through ultrasonic dispersion (40 kHz, 100 W) for 15 min, and the prepared Cu-MOF-74 stock

solution was shaken every 24 h before sampling. The sampled Cu-MOF-74 stock solution by centrifugation at 10 000 rpm for 20 min at room temperature. The collected supernatant was filtered through 0.22 μm filter, and then the concentration of Cu²⁺ released from Cu-MOF-74 (1 mg L⁻¹) in supernatant was measured by inductively coupled plasma emission spectrometer (Optima 8000, PerkinElmer, US). Based on the measured Cu²⁺ concentration, used CuSO₄·5H₂O as an additional ion, and to control the concentration of CuSO₄·5H₂O solution slightly higher than the equilibrium concentration of Cu²⁺ released by Cu-MOF-74 as a control group, then added equal amounts of the two solutions to the equal volume of algal cells suspension respectively. After that, shaking meanwhile sampling every 24 h, and the OD₆₈₀ values were analyzed by three-dimensional fluorescence spectrometer (EEMFS5, Edinburgh Instruments, UK).

2.3.2 Detection of cyanobacterial cell morphology. A blank control group was set, an algal cell suspension without adding Cu-MOF-74, and the experimental group was an algal cell suspension with Cu-MOF-74 that the concentration was 1 mg L⁻¹. After cultivated 48 h, the sampled algal cells suspension (50 mL) was centrifuged at 4500 rpm for 10 min and then added 10 mL 2.5% glutaraldehyde to settle for 2 h before centrifuged at 4500 rpm for 10 min again. The algal cells separated during the centrifugation were washed 3 times with distilled water and then dehydration was carried out with a series of concentrations (50%, 70%, 80%, 90%, and 95%) of anhydrous ethanol with the dehydration time interval of 15 min. After that, the algal cells were dehydrated with 100% anhydrous ethanol for 20 min and then immersed in it to cool in a refrigerator at 4 °C for 10 min. Subsequently, the sample supernatant was removed by filtration, and the algal cells were dried in a desiccator for 24 hours. The obtained algal cells were sprayed with gold and the cell morphology of algal cells were characterized by FESEM.

3 Result and discussion

3.1 Characterization of MOFs

3.1.1 Analysis of XRD. The XRD patterns of Cu-MOF-74, Zn-MOF-74, ZIF-8, Ag/AgCl@ZIF-8, and MIL-125(Ti) are shown in Fig. S1.† The diffraction peaks of Cu-MOF-74 and Zn-MOF-74 at the positions of 2θ = 6.8° and 11.8° were basically consistent with the theoretically calculated positions of MOF-74, indicating that Cu-MOF-74 and Zn-MOF-74 were successfully synthesized. In comparison with the results of Tanaka *et al.*,³² the diffraction peak of the ZIF-8 observed in XRD spectra with no obvious new diffraction peak appeared, indicating the synthesis of ZIF-8. Apparently, the Ag/AgCl@ZIF-8 sample not only maintains the original characteristic peaks of the ZIF-8 sample, but also shows the characteristic peaks of AgCl at the position of 2θ = 27.8°, 32.2°, 48.3°, and 54.5°, and the characteristic peak of crystal Ag³³ at position of 2θ = 38.1°, represented the synthesis of Ag/AgCl@ZIF-8. The diffraction peaks of MIL-125(Ti) at the positions of 2θ = 6.7°, 9.7°, 11.6°, 15.0°, 15.3°, 16.5°, 17.9°, 19.5°, and 25.0° were also basically corresponded to the theoretically calculated position of MIL-125(Ti), indicated synthesis of MIL-125(Ti).



3.1.2 Analysis of SEM. SEM images of Cu-MOF-74, Zn-MOF-74, ZIF-8, Ag/AgCl@ZIF-8, and MIL-125(Ti) were shown in Fig. S2.† It can be seen from Fig. S2† that for the same ligand, when doped with different metal ions, the morphology of the MOFs material would be different. For example, Cu-MOF-74 had a needle-like shape with a regular distribution, and the grain size was 3–4.5 μm , as a contrast, Zn-MOF-74 had no obvious shape and basically presented for the small particles agglomeration status; ZIF-8 showed a square shape with irregular edges, the crystal size of ZIF-8 was about 0.4 μm , and the distribution was relatively dispersed. But when ZIF-8 was doped with Ag^+ , the formed Ag/AgCl@ZIF-8 was a square crystal with different size and shape, and some of the crystals were in agglomerated stated with the relatively dense distribution; MIL-125(Ti) presented for the disk-shaped with a grain size of about 2 μm .

3.1.3 Analysis of XPS. In order to reveal the chemical states and element composition of five as-synthetic MOFs, XPS analyses were carried out.

From the survey scan spectrum in Fig. S3,† Ag/AgCl@ZIF-8 was composed by Zn, Ag, Cl, C, N and O elements. The binding energy sites of C 1s and N 1s in Ag/AgCl@ZIF-8 were at 284.55 eV and 398.65 eV respectively, and the bond energy sites of N 1s (398.65 eV) explain the existence of C–N bond and 2-methylimidazole.³⁴ The specific peaks of Ag 3d could be attributed to the Ag 3d_{3/2} (373.9 eV) and Ag 3d_{5/2} (367.9 eV), which on behalf of the presence of Ag^+ and Ag^0 ; the specific peaks of Zn 2p could be attributed to the Zn 2p_{3/2} (1021.25 eV) and Zn 2p_{1/2} (1044.3 eV), which were consistent with the exist of Zn^{2+} ; and the characteristic peak of Cl 2p were consisted by characteristic peaks of Cl 2p_{1/2} (198 eV) and Cl 2p_{3/2} (199 eV).³⁵ The above XPS results confirm the existed of ZIF-8 in Ag/AgCl@ZIF-8, which are accordant with XRD results.

From the survey scan spectrum in Fig. S4,† Zn-MOF-74 contains elements such as Zn, N, O, C, *etc.* The Zn 2p spectrum exhibits two contributions, Zn 2p_{3/2} and Zn 2p_{1/2}, located at respectively 1021.3 and 1044.3 eV, which can be assigned to Zn^{2+} .³⁵ The characteristic peaks of N 1s (400.5 eV), O 1s (531.75 eV), C 1s (284.5 and 288.5 eV) of Zn-MOF-74 were basically the same as Cu-MOF-74. However, the skewing of the characteristic peak position of N 1s, O 1s and C 1s and the newly added characteristic peak of C 1s may due to the formation of C=O (288.5 eV), C=C (284.6 eV), C=N (400.6 eV).

From the survey scan spectrum in Fig. S5,† the elemental composition of Cu-MOF-74 included Cu, N, O, and C. The coexistence of Cu^+ and Cu^{2+} in Cu-MOF-74 was evidenced by the main peak of Cu 2p_{1/2}, which was assigned to Cu^+ . The other main peak of Cu 2p_{3/2} and its shakeup satellite were due to Cu^{2+} .³⁶ And the N 1s (399.75 eV), O 1s (531.25 eV), C 1s (285 eV) spectrum clearly evidences the presence of organic acid (2,5-dihydroxyterephthalic acid). The above XPS results confirm the existed of MOF-74 in Cu-MOF-74, which are accordant with XRD results.

From the survey scan spectrum in Fig. S6,† the main elements of ZIF-8 were composed of Zn O, C, N, *etc.* The specific peaks of Zn 2p could be attributed to the Zn 2p_{3/2} (1021.3 eV) and Zn 2p_{1/2} (1044.3 eV), which were consistent with the exist of Zn^{2+} . The spectrum of C 1s, O 1s and N 1s demonstrated the

existence of C–N, C–C, C=O and 2-methylimidazole, which further confirmed the successful synthesis of ZIF-8.^{34,35}

From the survey scan spectrum in Fig. S7,† the elemental composition of MIL-125(Ti) included Ti, O, and C.³⁷ The Ti 2p spectrum of MIL-125(Ti) were observed at 458.8 eV and 464.5 eV, indicated that titanium combined with oxygen to remain in oxidation state IV.³⁸ The O 1s spectrum exhibited two peaks, located at 530.4 and 532.1 eV, can be ascribed to oxygen in titanium; the specific peaks of C 1s could be attributed to C–C (284.1 eV)³⁸ and C=O (288.1 eV). The above XPS results confirm the successful synthesis of MIL-125(Ti).³⁸

3.1.4 Stability analysis of MOFs. The release of metal ions situation by MOFs (1 mg L^{−1}) in water was shown in Fig. S8.† As can be seen from Fig. S8,† the five MOFs had good stability in water, shown as the less release of metal ions (below 0.3 mg L^{−1}) by MOFs in water during 6 days. According to the release of metal ions in water by five different species of MOFs, it can be found that the stability of five MOFs in water basically presented for MIL-125(Ti) > Cu-MOF-74 > Ag/AgCl@ZIF-8 > ZIF-8 > Zn-MOF-74. The stability of different species of MOFs in water was different. Compared with MOFs containing Ag^+ , Cu^{2+} and Ti^{4+} , the stability of MOFs only containing Zn^{2+} had obvious deficiency: after 1d, the metal ions released by Ag/AgCl@ZIF-8, Cu-MOF-74 and MIL-125(Ti) in the water was basically stable; however, the release of Zn^{2+} by ZIF-8 and Zn MOF-74 was continually increased until the fifth day. In addition, through the analysis of the Zn^{2+} mass loss in water for Ag/AgCl@ZIF-8, ZIF-8 and Zn-MOF-74, it can be speculated that Ag/AgCl@ZIF-8 can guarantee the release of a certain amount of Ag^+ , meanwhile, can effectively prevents the excessive loss of Zn^{2+} in water, showing higher stability and potential of algal removal.

3.2 Inhibition characterization of cyanobacterial using MOFs

3.2.1 Effects of MOFs species under different concentrations. The effect of different species of MOFs on the growth of algal cells at concentrations of 1, 5, and 10 mg L^{−1} are showed in Fig. 1. From the overall analysis of Fig. 1(a)–(c), when the concentration increased to 1 mg L^{−1}, five kinds of MOFs began to show inhibition of the growth of algal cells in different degree, and the inhibition rate increased with the increase of MOFs concentration. After 24 h, Cu-MOF-74 had exhibited the most excellent inhibitory performances for algal cell among the five MOFs, and the inhibitory rate of the five materials on algae cells basically presented for Cu-MOF-74 > Ag/AgCl@ZIF-8 > ZIF-8 > Zn-MOF-74 > MIL-125(Ti). In addition, comparing the inhibitory effects of Cu-MOF-74 and Zn-MOF-74, Ag/AgCl@ZIF-8 and ZIF-8, it was found that MOFs containing Cu^{2+} and Ag^+ had significant destruction capacity for algal cells than those containing Zn^{2+} . But the effect of organic ligand species in MOFs on the growth of algal cells was not as obvious as metal ions, only when the concentration of MOFs was more than 5 mg L^{−1}, could be found that MOFs containing the ligand GC had better power of algal removal than that containing the ligand DHTA.

The above results showed that when algal cells were exposed to each MOFs, of which the concentration reached a certain



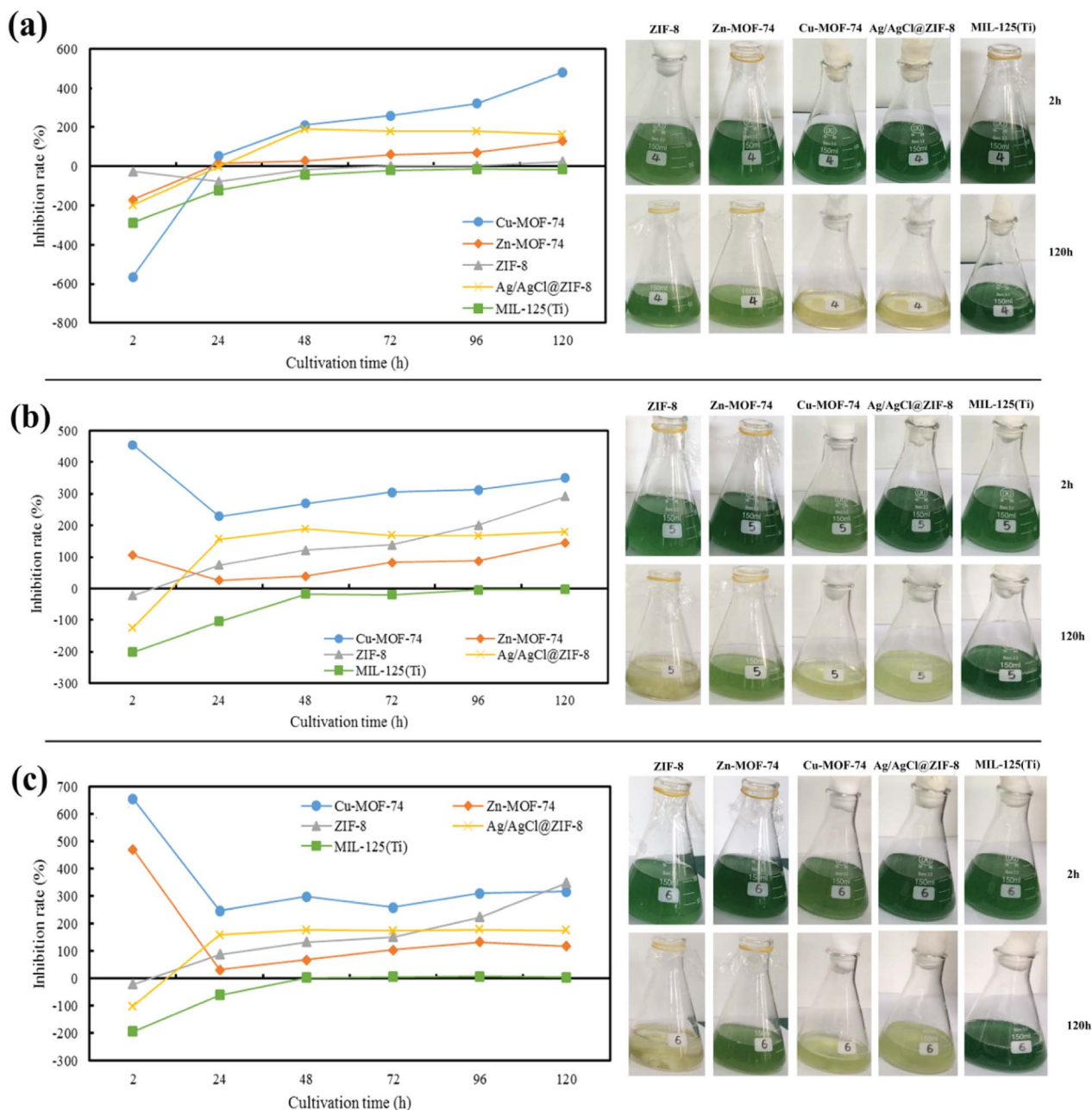


Fig. 1 Effects of MOFs on algae under different concentrations: (a) 1 mg L⁻¹, (b) 5 mg L⁻¹, (c) 10 mg L⁻¹.

threshold, the growth of algal cells will be inhibited in different degrees. It may be because the distinct of interaction between different types of metal ions and ligands existed in MOFs caused the different dissolving quantity and releasing rate³⁹ of metal ions from MOFs in aqueous solutions. In addition, the toxicity of these MOFs mainly depended on the dissolved metal ions, and the sensitivity of *M. aeruginosa* to different metal ions dissolved in water was different. Just as Cu-MOF-74 had the best algal inhibition ability, probably due to the presence of phycocyanin in *M. aeruginosa* which was extremely sensitive to Cu²⁺.

3.2.2 Modeling of growth kinetics. The kinetic model has been widely used to explain the growth kinetics of

nanomaterials inhibit of algal cells. In this study, the concentration of 10 mg L⁻¹ Cu-MOF-74 was used to treat *M. aeruginosa*, and the growth kinetics discipline of inhibition of algal cells by MOFs was explored by fitting with pseudo-first-order kinetics model and pseudo-second-order kinetics model. The two fitting curves of inhibition of algal cells by MOFs are shown in Fig. 2.

By comparing the pseudo-first-order kinetic model ($S_1^2 = 4.06 \times 10^{-4}$, $R_1^2 = 0.944$) and the pseudo-second-order kinetic model ($S_2^2 = 2.48 \times 10^{-4}$, $R_2^2 = 0.966$), it was found that inhibition of growth of *M. aeruginosa* by MOFs primarily followed the pseudo-second-order kinetics fitting model and the reaction equation was $C_{A2} = \frac{0.38893}{1 + 0.0098t}$.



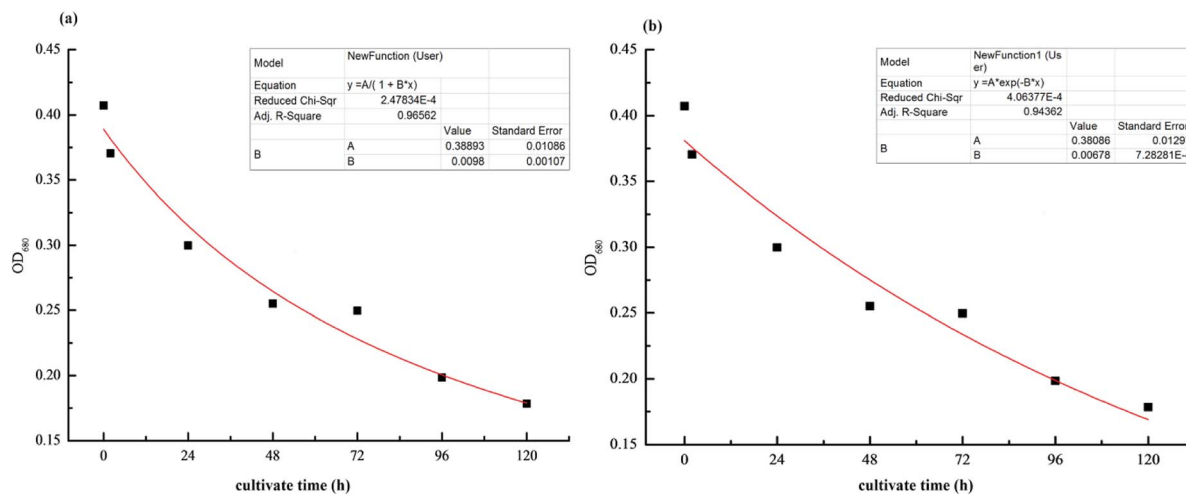


Fig. 2 Growth kinetic model for the inhibition of *M. aeruginosa* at a concentration of 10 mg L^{-1} Cu-MOF-74: (a) quasi-secondary-order growth kinetic mode. (b) Quasi-first-order growth kinetic model.

3.3 Inhibition characterization of cyanobacterial using ligands

The effect of ligand concentration on algal cells is shown in Fig. 3. The experimental results are consistent with the experimental results of Keila Martín-Betancor *et al.*²⁶ Compared with

the control group (0 mg L^{-1}), the ligands (DHTA, PTA, GC) all have a no-significant inhibitory effect on algae, which is merely performed by a decrease in the proliferation rate of the algae cells. Low concentration of ligand (1 mg L^{-1}) has indistinctly effect on algae cells, even at a concentration of 1 mg L^{-1} , DHTA promoted the growth of algae cells, but as the dosage of ligands

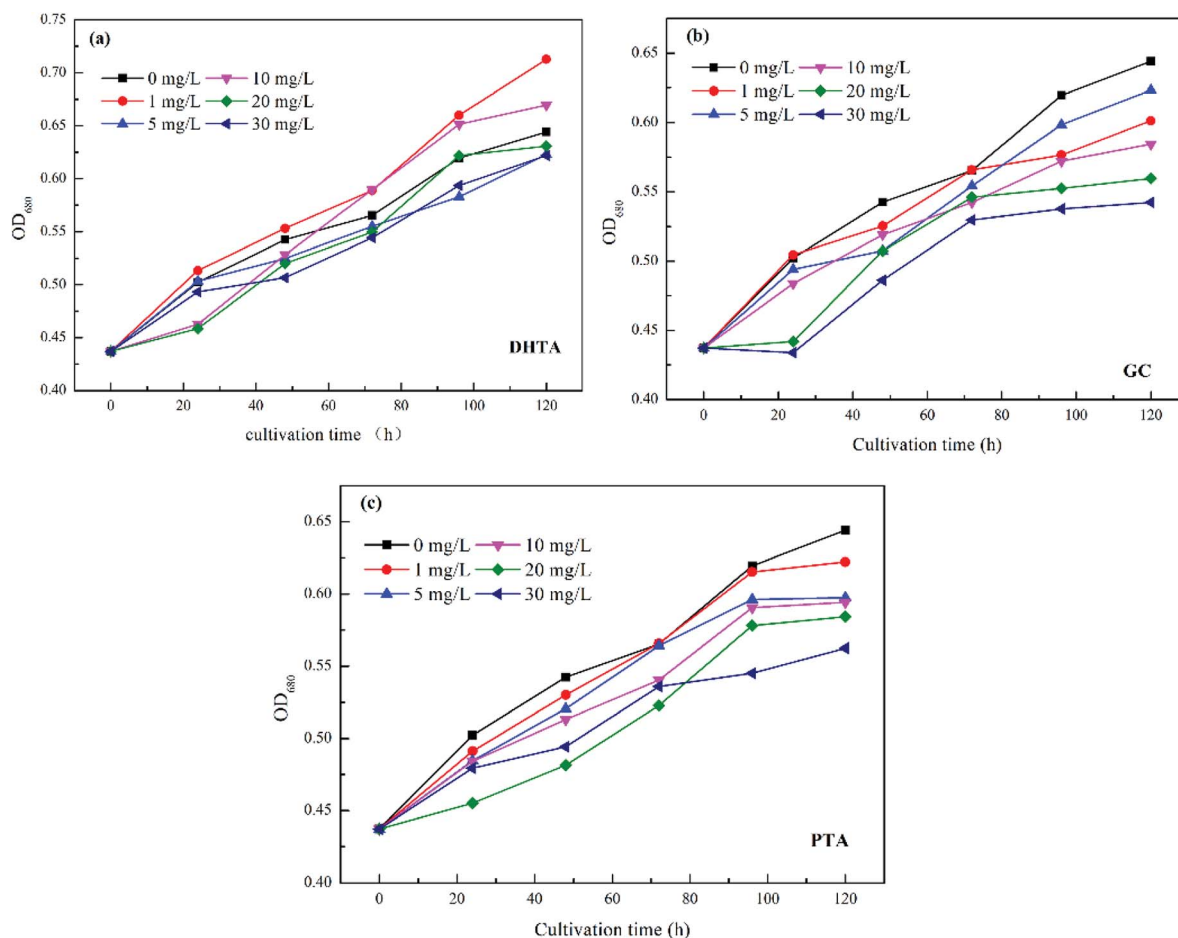


Fig. 3 Effects of different concentrations of ligands on algae cells: (a) DHTA, (b) GC, (c) PTA.



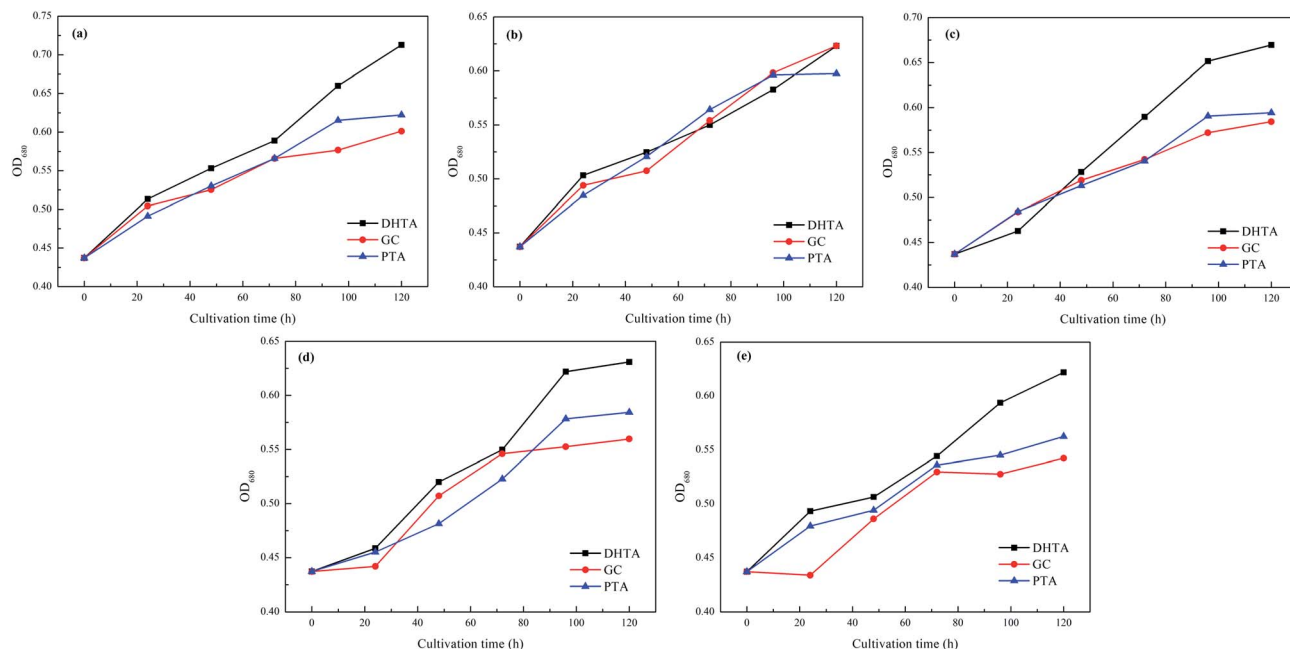


Fig. 4 Effect of ligand species on algae under different ligand concentrations: (a) 1 mg L^{-1} , (b) 5 mg L^{-1} , (c) 10 mg L^{-1} , (d) 20 mg L^{-1} , (e) 30 mg L^{-1} .

was further increased, the growth of algae cells was further inhibited.

And the effect of ligand species on algal cells is shown in Fig. 4. It can be seen that the inhibitory rate of the three ligands on algae cells basically presented for $\text{DHTA} < \text{PTA} < \text{GC}$. The distinction in the effect of the ligand to inhibit algal cells may be caused by the different solubility of the ligand, which was exhibiting the rule of $\text{DHTA} < \text{PTA} < \text{GC}$.

3.4 Comparative experiment on the algae inhibition effect between Cu-MOF-74, P25 and metal ions

The effects of Cu-MOF-74, metal ions (Ag^+ , Cu^{2+} , Zn^{2+}) and P25 on inhibiting algal cells were shown in Fig. 5. It can be seen from Fig. 5 that under the same ion concentration (1 mg L^{-1}), Zn^{2+} as well as P25 have almost no inhibition on algae cells, however, Ag^+ and Cu^{2+} had significant inhibitory effects on algae cells. But comparing to Ag^+ , Zn^{2+} , Cu^{2+} and P25, Cu-MOF-74 (1 mg L^{-1}) still has superior algae-inhibiting effect, especially when treated with Cu-MOF-74 (1 mg L^{-1}) for 120 h, the relative value of OD_{680} of algae cell suspension is reduced to 0.2 or so.

The above results showed that even in the absence of photocatalysis, the algae removal capacity of MOFs was more significant than that of ordinary nanomaterials, meanwhile, compared with the metal ions (Ag^+ and Cu^{2+} , Zn^{2+}), MOFs still have higher algae removal efficiency.

3.5 Effect of Cu-MOF-74 concentration on *M. aeruginosa*

The OD_{680} , Zeta potential and chroma of algal cells can reflect the inhibition of *M. aeruginosa* by Cu-MOF-74. After exposing to Cu-MOF-74 at concentrations of 0, 0.01, 0.05, 0.1, 1, 5, and 10 mg L^{-1} , the change of chroma, OD_{680} values, and Zeta potentials of algal cell suspensions over time are shown in Fig. 6

respectively. The Fig. 6(c) shows that the Zeta potential of the algal cell solution in the control group remains unchanged from 0 to 120 h, and the OD_{680} value of the algal cell solution gradually increases as the color of algal cell solution became deeper, indicating that the algal cells in the control group grow well (Fig. 6(a) and (b)). The tests treated with the concentration of $0.01\text{--}0.1 \text{ mg L}^{-1}$ Cu-MOF-74 show no significant change in the chroma, OD_{680} value and Zeta potential value of the algal cell solution compared to the control group. At 96 h, after being treated with 0.1 mg L^{-1} Cu-MOF-74, the OD_{680} value of algal cell for the experimental groups was even greater than that of the control group; meanwhile, at 96 and 120 h, Zeta potential value was also larger than that of the control group when contacted with Cu-MOF-74 of 0.05 and 0.1 mg L^{-1} , and the results were consistent with the change of OD_{680} values. It is presumed that

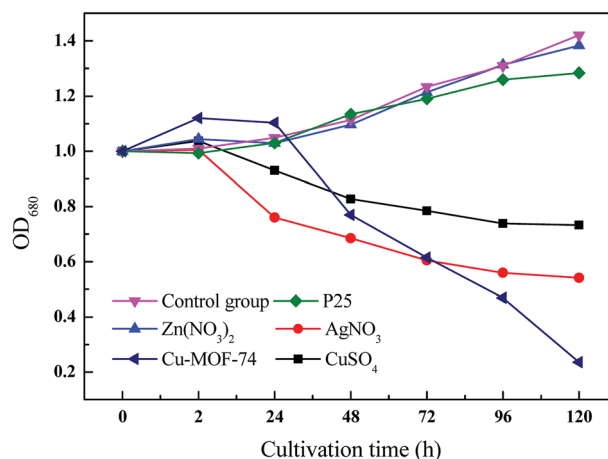


Fig. 5 Change of OD_{680} relative value of algal cell suspension treated by 1 mg L^{-1} P25; $\text{Zn}(\text{NO}_3)_2$; AgNO_3 ; Cu-MOF-74; CuSO_4 .



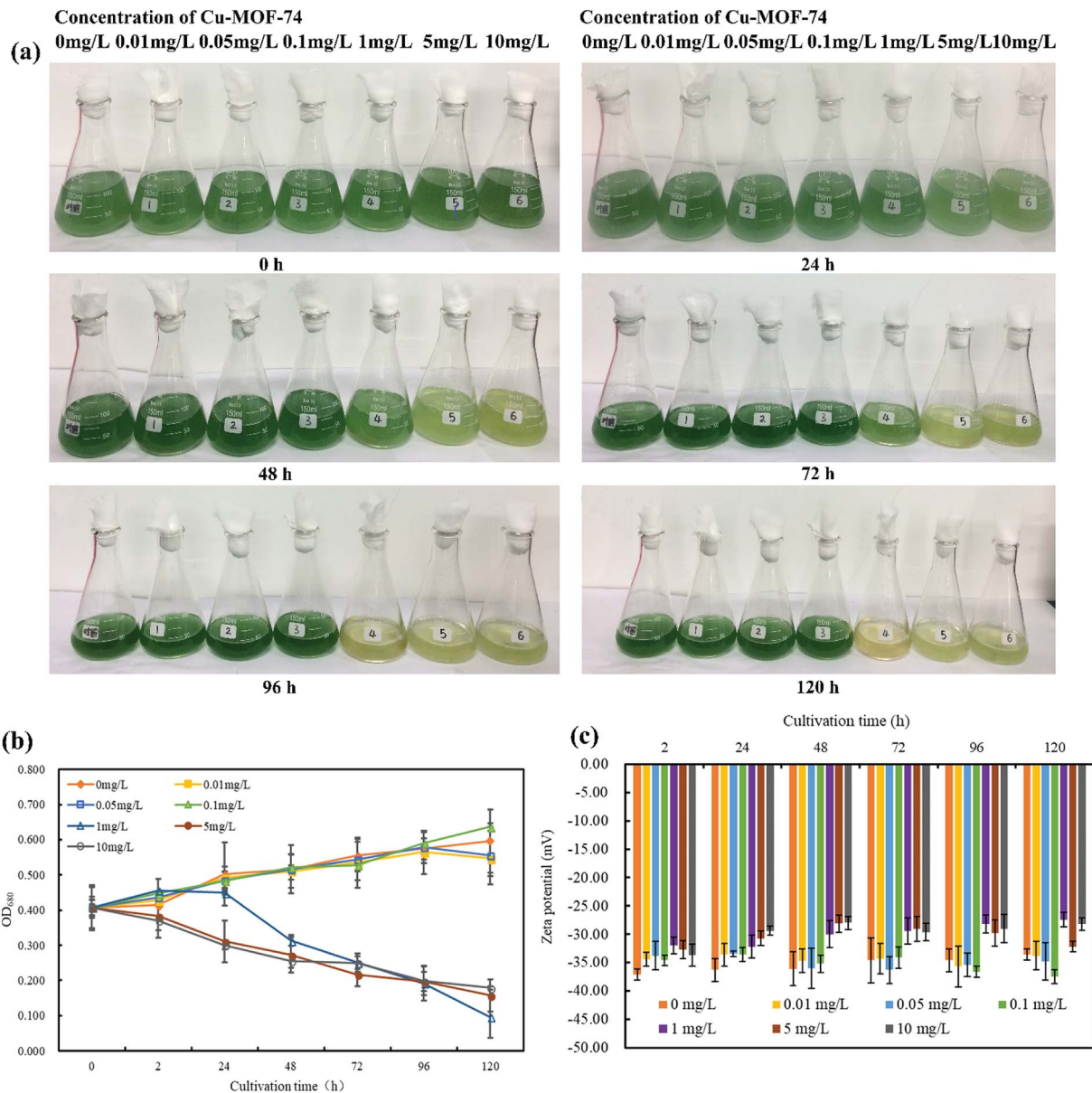


Fig. 6 (a) The effect of Cu-MOF-74 concentration on the chroma change of algal cell suspension. (b) The effect of Cu-MOF-74 concentration on algal cell OD_{680} . (c) The effect of Cu-MOF-74 concentration on Zeta potential of algal cell suspension.

maybe the lower concentration of MOFs stimulates the activity of certain enzymes inside the algae cells, which made the growth of the algal cells more exuberant. The experimental results were consistent with other studies, Duong *et al.*⁴⁰ through the experiment of nano-Ag to inhibit the growth of *M. aeruginosa* to find that the concentration of 0.001 mg L^{-1} nano-Ag can't inhibit the growth of algae cells; Mou *et al.*⁴¹ carried on experiment by using different types of carbon nanotubes to inhibit the *M. aeruginosa* to find that the growth of algal cells were also promoted when the concentration of carbon nanotubes was at a low dosage (0.1 to 1 mg L^{-1}).

When exposed to the concentration of 1 mg L^{-1} Cu-MOF-74, the OD_{680} value of algae cells increased firstly and then decreased as culture time went by. It was presumed that maybe the enzymatic activity of the algal cells was stimulated when the

Cu-MOF-74 was added, and the intracellular stress response promoted the increase of the density of the algal cells, but algal cells couldn't resist the stimulation brought by the Cu-MOF-74 continuously, as a result, the OD_{680} value of the algae cells gradually decreased at the end. Once the concentration of Cu-MOF-74 above 1 mg L^{-1} , the absolute values of OD_{680} and Zeta potential of algal cells decreased significantly with the increase of treatment time, meanwhile, the chroma of algae solution was dimmed in different degrees, and there was no trend of recovery growth for algal cells during the incubation period of 5 d.

The above experimental results clearly demonstrated that the concentration of Cu-MOF-74 can affect the growth of algal cells. When the concentration reached a threshold (1 mg L^{-1}), Cu-MOF-74 will start to suppress algal cells, and the inhibitory



effect will become stronger as the concentration of Cu-MOF-74 increased, presented for the significantly dimmed of chroma of the algal cell solution, the decrease of OD₆₈₀ and Zeta potential value of the algal cell solution.

3.6 Physiological characterization of cyanobacterial using Cu-MOF-74

3.6.1 Index of extracellular TOC. The extracellular TOC content of algal cells is one of the indicators for characterizing the physiological characteristics of algal cells. After different concentrations of Cu-MOF-74 were used to treat algal cells, the changes in extracellular TOC content of algal cells with culture time were shown in Fig. 7(B). When the algal cells were exposed to the concentrations of 0.01, 0.05 and 0.1 mg L⁻¹ Cu-MOF-74, the extracellular TOC content of the algal cells was not significantly different from that of the control group within 0–72 h, while the concentration of Cu-MOF-74 reached at 1, 5 and 10 mg L⁻¹ with the treatment time for 2 h, the TOC content of the algal cells in the experimental group was higher than that of the control group already. Subsequently, the TOC content of the

algal cells began to increase rapidly after 2 h, and at the end of 24 h, the TOC content of the algal cells in the experimental groups increased by 5.64, 9.97, and 11.66 mg L⁻¹, respectively. It was inferred that maybe the algal cells damaged due to the attack from Cu-MOF-74 (1, 5, and 10 mg L⁻¹) with the increase of the treatment time, resulted in the leakage of intracellular substances such as humic acids and fulvic acids, which was in accordance with the TOC content measurement result. The relevant document demonstrated similar experimental results, Xuejiang Wang *et al.*⁴² found that after algae were treated by floating nano-materials (F-Ce-TiO₂/EP450) for 4 hours, accompanied with algal cells damaged, humic acids released outside the algal cells. But at 48 h, the TOC content of the algal cells didn't increase continually, that be related to the adsorption of TOC for Cu-MOF-74.

3.6.2 Index of cell membrane integrity. The algal cell membrane integrity is another physiological characteristic indicator of algal cells. The cell membrane integrity of algal cells treated for 24 h with different concentrations of Cu-MOF-74 was examined to explore whether Cu-MOF-74 would affect the integrity of algal cell membranes. The flow cytometry

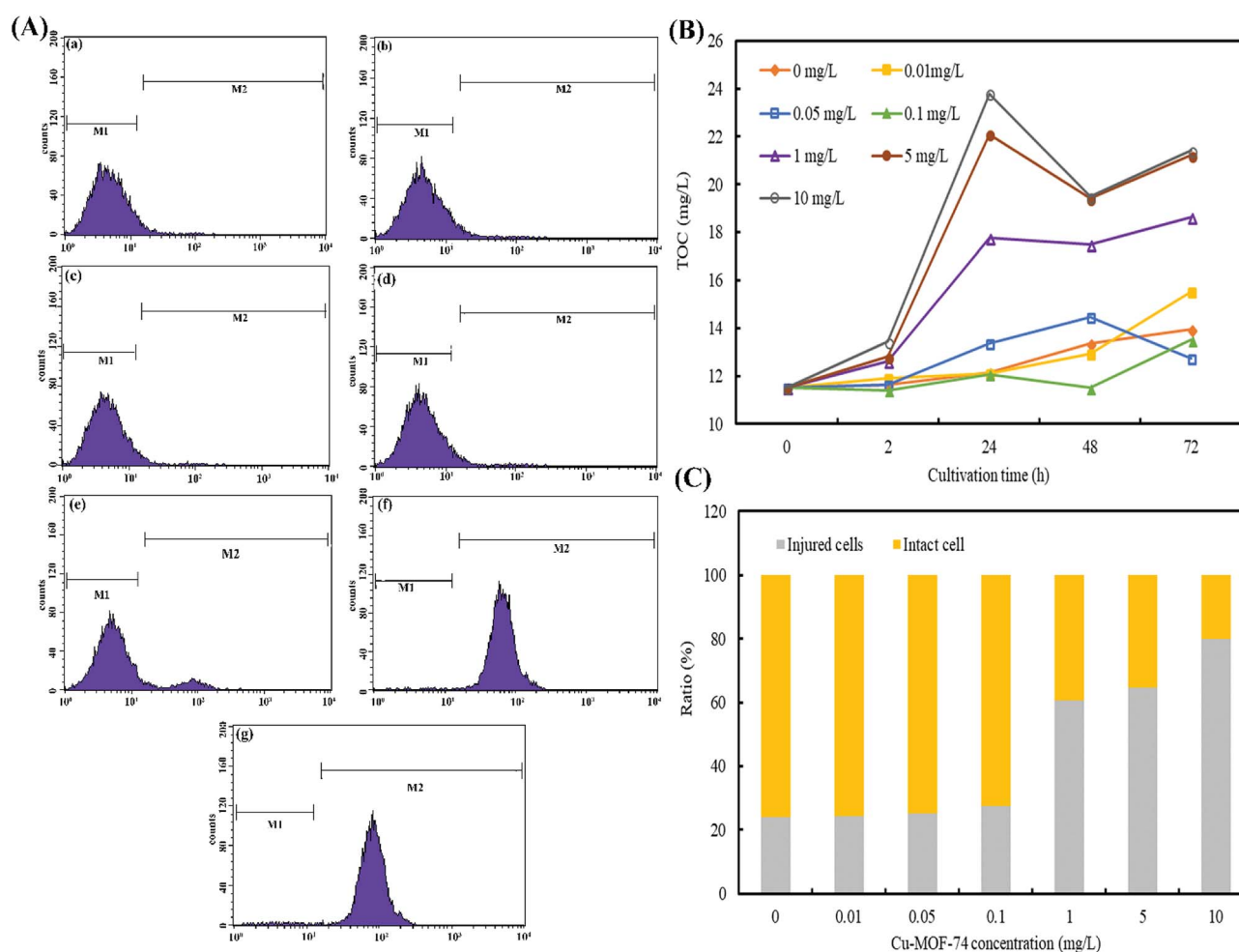


Fig. 7 (A) Flow cytometry spectra of algae cells treated with different concentrations of Cu-MOF-74 for 24 h: (a) 0 mg L⁻¹, (b) 0.01 mg L⁻¹, (c) 0.05 mg L⁻¹, (d) 0.1 mg L⁻¹, (e) 1 mg L⁻¹, (f) 5 mg L⁻¹, (g) 10 mg L⁻¹. (B) Effect of Cu-MOF-74 concentration on extracellular TOC content of algal cells. (C) Changes of cell membrane integrity of algae treated with Cu-MOF-74 at different concentrations for 24 h.



detection spectrum of algal cells treated with different concentrations of Cu-MOF-74 for 24 h were shown in Fig. 7(A).

M1 region was defined as a living cell region and M2 as a damaged cell region. When algal cells in experimental group were treated with Cu-MOF-74 ($0.01\text{--}0.1\text{ mg L}^{-1}$), the PI fluorescence intensity of them was mainly concentrated in the M1 region, which was not significantly different from the control group. The results obviously demonstrated that Cu-MOF-74 with the low concentration ($<0.1\text{ mg L}^{-1}$) did not cause significant damage to the algal cells. However, once the concentration of Cu-MOF-74 increased to 1 mg L^{-1} , the PI fluorescence in the M2 region began to increase, which manifested the severe cell structure damaged of algal cells. And the PI fluorescence intensity in the M2 region showed a further increase trend which goes with the increase of the concentration of Cu-MOF-74.

The Fig. 7(C) showed that the algal cells without any treatment in the control group produced 24.03% of the naturally-damaged cells. Treated with Cu-MOF-74 ($0.01, 0.05$, and 0.1 mg L^{-1}) for 24 h, the proportion of damaged *M. aeruginosa* cells was not significantly different from that of the control group, but the proportion of damaged cells increased dramatically when treated with Cu-MOF-74 ($1, 5$, and 10 mg L^{-1}), and the damaged cells reached to 60.65%, 64.56%, and 79.84%, respectively. The phenomenon reflected that once the concentration of Cu-MOF-74 reached the threshold, the integrity of algal cells would be destructed, which damaged the algal cells.

3.7 Proposed cyanobacterial inhibition mechanisms of Cu-MOF-74

3.7.1 Effects of Cu^{2+} . The toxicity of nanomaterials to algal cells is strongly mediated by the dissolved metal ions released from them. Miao *et al.*²⁵ found that the released Ag^+ from nano-Ag led to the growth inhibition of the *Thalassiosira weissflogii*; Aruoja *et al.*⁴³ found that nano-ZnO, nano- TiO_2 , and nano-CuO had inhibitory effect on *Monilia* sp., and they believed that the growth suppression of *Monilia* contributed to the metal ions released from nano metal oxide particle. In order to further explore whether the destruction of algal cells by MOFs was due to the metal ions entirely, we performed tests to determine the effect of Cu-MOF-74 on the growth of algal cells whether depended on the Cu^{2+} released from it totally. The concentration of Cu^{2+} released from Cu-MOF-74 (1 mg L^{-1}) was shown in Fig. 8(c), the change of OD_{680} values of algal cell suspension after treated by $0.21\text{ mg L}^{-1}\text{ CuSO}_4\cdot 5\text{H}_2\text{O}$ and $1\text{ mg L}^{-1}\text{ Cu-MOF-74}$ was shown in Fig. 8(a), and the comparison of inhibition rates of algal cells by Cu-MOF-74 (1 mg L^{-1}) and $\text{CuSO}_4\cdot 5\text{H}_2\text{O}$ (0.21 mg L^{-1}) was shown in Fig. 8(b).

From Fig. 8(a) and (c), Cu^{2+} released from $1\text{ mg L}^{-1}\text{ Cu-MOF-74}$ increased continuously from 2 to 48 h, and the amount of Cu^{2+} released reaches equilibrium (0.21 mg L^{-1}) after 48 h. According to the concentration of Cu^{2+} released from $1\text{ mg L}^{-1}\text{ Cu-MOF-74}$ dissolved in water, $0.21\text{ mg L}^{-1}\text{ CuSO}_4\cdot 5\text{H}_2\text{O}$ was selected as the Cu^{2+} external additive. Through comparative analysis, it could be seen that the OD_{680} value of the algal cell

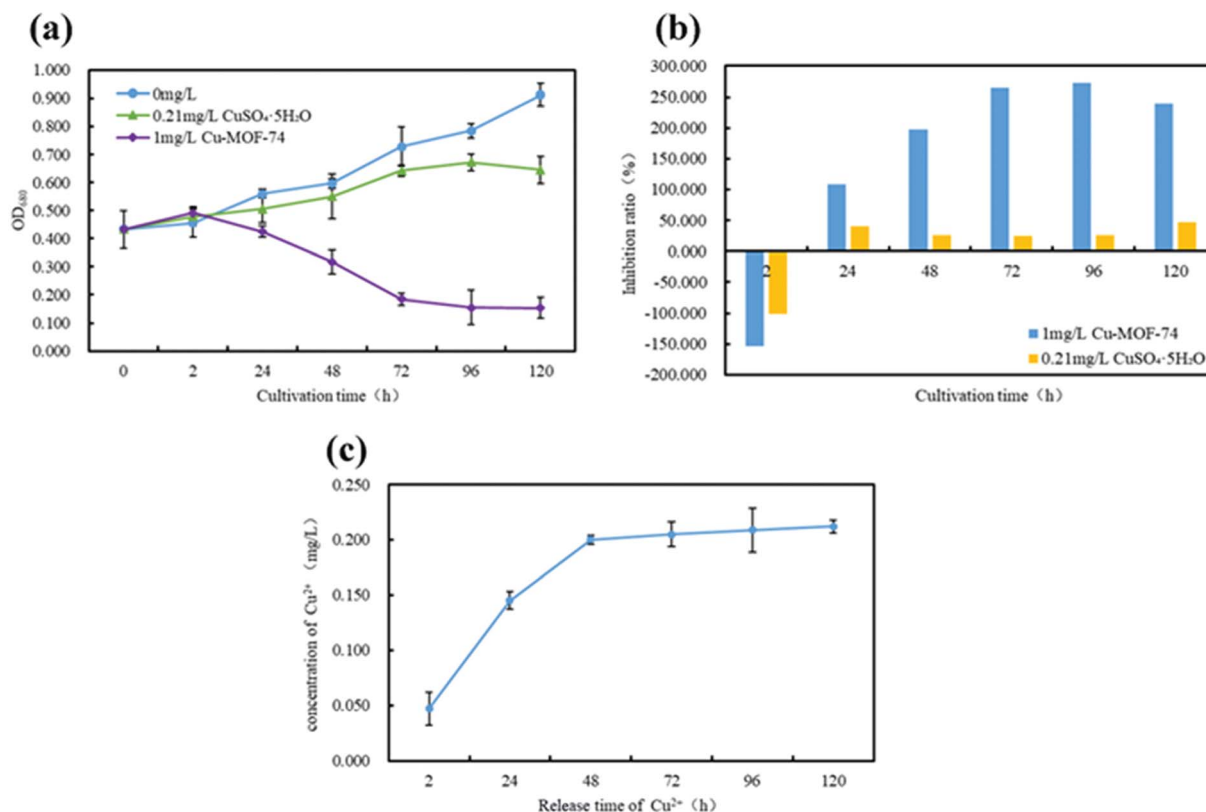


Fig. 8 (a) Change of OD_{680} values of algal cell suspension treated by $0.21\text{ mg L}^{-1}\text{ CuSO}_4\cdot 5\text{H}_2\text{O}$ and $1\text{ mg L}^{-1}\text{ Cu-MOF-7}$. (b) Comparison of inhibition rates of algal cell by $1\text{ mg L}^{-1}\text{ Cu-MOF-74}$ and $0.21\text{ mg L}^{-1}\text{ CuSO}_4\cdot 5\text{H}_2\text{O}$. (c) Change of Cu^{2+} concentration released by $1\text{ mg L}^{-1}\text{ Cu-MOF-74}$.



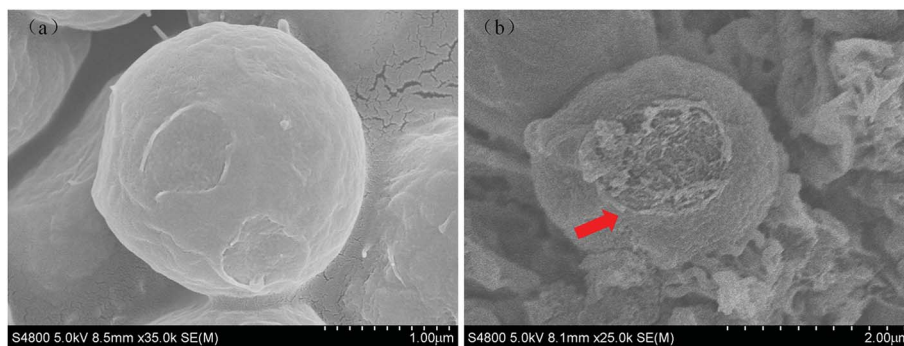


Fig. 9 SEM images of algal cells in control and experimental groups (1 mg L^{-1} Cu-MOF-74) after 48 h treatment: (a) control group, (b) experimental groups.

suspension added with Cu-MOF-74 was always lower than that added with $\text{CuSO}_4 \cdot 5\text{H}_2\text{O}$.

From Fig. 8(b), compared with $\text{CuSO}_4 \cdot 5\text{H}_2\text{O}$ (0.21 mg L^{-1}), the Cu-MOF-74 (1 mg L^{-1}) had exhibited excellent performances for killing algal cells. At 96 h, the Cu-MOF-74 had achieved the maximum relative inhibition rate of algal cells (272.74%), but the maximum relative inhibition rate of $\text{CuSO}_4 \cdot 5\text{H}_2\text{O}$ to algae cells was only 39.98% during 0–120 h. It was obviously shown that the suppression ability of Cu-MOF-74 to algae was better than $\text{CuSO}_4 \cdot 5\text{H}_2\text{O}$, suggesting that Cu-MOF-74 released Cu^{2+} was only a part of factor that inhibited the growth of algal cell. Related document has got similar conclusions, Zhang *et al.*⁴⁴ found that the inhibition rate of nano-CuO for *Chlorella* was consistently higher than that of Cu^{2+} during experimental culture; Ji *et al.*⁴⁵ found that both nano- TiO_2 and nano-ZnO have an impact on the growth of *Chlorella*, and the inhibition mechanism of nano-ZnO on *Chlorella* was mainly based on the effect of Zn^{2+} and the oxidative damage of algae by ROS *etc.* Based on the experimental results, it was presumed that the inhibition mechanism of Cu-MOF-74 may have other causes besides the effect of Cu^{2+} .

3.7.2 Effect of Cu-MOF-74 on the morphology of cyanobacteria. In the study of physiological characteristics of algal cells, it was found that the extracellular TOC content of the solution increased with the addition of Cu-MOF-74, which may due to the destruction of cell integrity by Cu-MOF-74. In order to further determine whether Cu-MOF-74 had an effect on the morphology of algal cells, the algal cells treated with Cu-MOF-74 (1 mg L^{-1}) for 48 hours were observed by SEM, and the SEM images of algal cells in the control and experimental groups were shown in Fig. 9.

In Fig. 9(a), the algal cells in the control group were intact and the cell wall surface, presented for a complete elliptical shape, was smooth which indicated their healthy status. Fig. 9(b) showed the SEM image of algal cells after being treated with 1 mg L^{-1} Cu-MOF-74 for 48 h. Due to the cell wall support, the cells still kept their basic shape, but the morphology of the algal cells was changed: the cell wall edges were not smooth and began to shrink accompanied with pits appeared on the surface of algal cell, indicating the damage of algal cells in the experimental group. It was presumed that the damage of algal cells

may be caused by the Cu-MOF-74 or its released Cu^{2+} adsorbed on its surface. For example, Lin⁴⁶ *et al.* observed that TiO_2 was adsorbed on the surface of *Chlorella*; Chen⁴⁷ *et al.* found that when the effect concentration of TiO_2 reached 100 mg L^{-1} , a large amount of TiO_2 would adsorbed on the cell wall surface of *Reinhardtii. sp.*

4 Conclusion

The five MOFs in this study all had good stability in water and the order of stability of MOFs in water basically display as MIL-125(Ti) > Cu-MOF-74 > Ag/AgCl@ZIF-8 > ZIF-8 > Zn-MOF-74. When the concentration of MOFs such as Cu-MOF-74, Ag/AgCl@ZIF-8, Zn-MOF-74, ZIF-8 and MIL-125(Ti) reached the threshold, all of them were demonstrated to be effective for the removal of algal cells in different degrees. Both the species of metal ions and organic ligands will affect the inhibitory effect of MOFs, however, the activity presented by MOFs is mainly depended on the metal ions released from them. The inhibitory effect of MOFs containing Cu^{2+} and Ag^+ on algal cells is better than that of MOFs containing Zn^{2+} ; the inhibitory effect of MOFs containing organic ligand GC on algal cells is better than that of organic ligands DHTA. The order of the inhibitory effects of five MOFs on *M. aeruginosa* from stronger to weaker is Cu-MOF-74 > Ag/AgCl@ZIF-8 > ZIF-8 > Zn-MOF-74 > MIL-125(Ti). In addition, the concentration of Cu-MOF-74 is proved to be one of the mainly factors affecting the growth of algal cells since the concentration of Cu-MOF-74 reached the threshold (1 mg L^{-1}), the growth of algal cells will be inhibited. With the increase of the concentration of Cu-MOF-74, the OD_{680} value, Zeta potential and chroma of the algal cell suspension continued to decrease as the culture time increased, indicating that the growth inhibition of algal cells, and the growth inhibition reaction of *M. aeruginosa* by Cu-MOF-74 followed the pseudo-second-order kinetics fitting mode. The metal ions released by the MOFs would damage the algal cell membranes, causing the destruction of cell integrity of the algal cells in different degrees. As a result, the contents of the algal cells would flow out and the TOC content of the extracellular cells would increase to varying degrees. Meanwhile, it would also lead to the gradual decrease of the Zeta potential of the algal cell



suspension. Then the algal cells would cause aggregation and precipitation due to poor stability which achieved the purpose of suppressing algae.

Conflicts of interest

There are no conflicts to declare.

Acknowledgements

The authors would like to gratefully acknowledge the financially support from the National Natural Science Foundation of China (No. 51778146), the Outstanding Youth Fund of Fujian Province in China (No. 2018J06013), the China Postdoctoral Science Foundation (No. 2014M561856), and the Open test fund for valuable instruments and equipment of Fuzhou University (No. 2018T033).

References

- 1 B. E. Lapointe, L. W. Herren, D. D. Debortoli and M. A. Vogel, *Harmful Algae*, 2015, **43**, 82–102.
- 2 J. D. Isaacs, W. K. Strangman, A. E. Barbera, M. A. Mallin, M. R. Mciver and J. L. C. Wright, *Harmful Algae*, 2014, **31**, 82–86.
- 3 M. A. Burford, S. A. Johnson, A. J. Cook, T. V. Packer, B. M. Taylor and E. R. Townsley, *Water Res.*, 2007, **41**, 4105–4114.
- 4 G. M. Hallegraeff, *Phycologia*, 1993, **32**, 79–99.
- 5 W. W. Carmichael, W. R. Evans, Q. Q. Yin, P. Bell and E. Moczydlowski, *Appl. Environ. Microbiol.*, 1997, **63**, 3104–3110.
- 6 E. M. Jochimsen, W. W. Carmichael, J. S. An, D. M. Cardo, S. T. Cookson, C. E. Holmes, M. B. Antunes, D. M. F. Da, T. M. Lyra and V. S. Barreto, *N. Engl. J. Med.*, 1998, **338**, 873–878.
- 7 G. Fan, W. Chen, Z. Su, R. Lin, R. Xu, X. Lin and Q. Zhong, *Desalin. Water Treat.*, 2017, **68**, 70–79.
- 8 J. Plummer, *J. Water Supply: Res. Technol.-AQUA*, 2002, **51**, 307–318.
- 9 J. Nimptsch, C. Wiegand and S. Pflugmacher, *Environ. Sci. Technol.*, 2008, **42**, 8552.
- 10 G. Zhang, P. Zhang and M. Fan, *Ultrason. Sonochem.*, 2009, **16**, 334–338.
- 11 L. Garc a A-Villada, M. Rico, M. M. Altamirano, N. N. L. S a, V. L a Pez-Rod as and E. Costas, *Water Res.*, 2004, **38**, 2207–2213.
- 12 S. Zhou, Y. Shao, N. Gao, L. Li, J. Deng, M. Zhu and S. Zhu, *Sci. Total Environ.*, 2014, **482–483**, 208–213.
- 13 F. D. Hulot, G. Lacroix, F. Lescher-Moutou   and M. Loreau, *Nature*, 2000, **405**, 340.
- 14 A. G. Slater and A. I. Cooper, *Science*, 2015, 348.
- 15 Q. L. Zhu and Q. Xu, *Chem. Soc. Rev.*, 2014, **43**, 5468–5512.
- 16 N. M. Franklin, N. J. Rogers, S. C. Apte, G. E. Batley, G. E. Gadd and P. S. Casey, *Environ. Sci. Technol.*, 2007, **41**, 8484–8490.
- 17 C. Yang, X. You, J. Cheng, H. Zheng and Y. Chen, *Appl. Catal., B*, 2017, **200**, 673–680.
- 18 C. Saison, F. Perreault, J. C. Daigle, C. Fortin, J. Claverie, M. Morin and R. Popovic, *Aquat. Toxicol.*, 2010, **96**, 109–114.
- 19 M. H. Park, K. H. Kim, H. H. Lee, J. S. Kim and S. J. Hwang, *Biotechnol. Lett.*, 2010, **32**, 423–428.
- 20 A. Kubacka, N. A. M. Fern   and G. Col   N, *Chem. Rev.*, 2012, **112**, 1555–1614.
- 21 M. Zhao, K. Yuan, Y. Wang, G. Li, J. Guo, L. Gu, W. Hu, H. Zhao and Z. Tang, *Nature*, 2016, **539**, 76.
- 22 R. Chandra, S. Mukhopadhyay and M. Nath, *Mater. Lett.*, 2016, **164**, 571–574.
- 23 C. Yang, X. You, J. Cheng, H. Zheng and Y. Chen, *Appl. Catal., B*, 2017, **200**, 673–680.
- 24 Y. Liu, J. Zhan and Y. Hong, *Environ. Sci. Pollut. Res.*, 2017, **24**, 26594–26604.
- 25 A. Miao, K. A. Schwehr, C. Xu, S. Zhang, Z. Luo, A. Quigg and P. H. Santschi, *Environ. Pollut.*, 2009, **157**, 3034–3041.
- 26 K. Mart  n-Betancor, S. Aguado, I. Rodea-Palomares, M. Tamayo-Belda, F. Legan  s, R. Rosal and F. Fern  ndez-Pi  as, *Sci. Total Environ.*, 2017, **595**, 547–555.
- 27 N. Gu, J. Gao, K. Wang, B. Li, W. Dong and Y. Ma, *J. Taiwan Inst. Chem. Eng.*, 2016, **64**, 189–195.
- 28 R. Sanz, F. Mart  nez, G. Orcajo, L. Wojtas and D. Briones, *Dalton Trans.*, 2013, **42**, 2392–2398.
- 29 Y. Tang, J. Tian, S. Li, C. Xue, Z. Xue, D. Yin and S. Yu, *Sci. Total Environ.*, 2015, **532**, 154–161.
- 30 G. Fan, W. Chen, Z. Su, R. Lin, R. Xu, X. Lin and Q. Zhong, *Desalin. Water Treat.*, 2017, **68**, 70–79.
- 31 X. Wu, E. M. Joyce and T. J. Mason, *Water Res.*, 2012, **46**, 2851–2858.
- 32 S. Tanaka, K. Kida, M. Okita, Y. Ito and Y. Miyake, *Chem. Lett.*, 2012, **41**, 1337–1339.
- 33 S. T. Gao, W. H. Liu, N. Z. Shang, C. Feng, Q. H. Wu, Z. Wang and C. Wang, *RSC Adv.*, 2014, **4**, 61736–61742.
- 34 J. Liu, R. Li, Y. Hu, T. Li, Z. Jia, Y. Wang, Y. Wang, X. Zhang and C. Fan, *Appl. Catal., B*, 2017, **202**, 64–71.
- 35 G. Fan, X. Zheng, J. Luo, H. Peng, H. Lin, M. Bao, L. Hong and J. Zhou, *Chem. Eng. J.*, 2018, **351**, 782–790.
- 36 R. Sanz, F. Mart  nez, G. Orcajo, L. Wojtas and D. Briones, *Dalton Trans.*, 2013, **42**, 2392–2398.
- 37 H. Wang, X. Yuan, Y. Wu, G. Zeng, X. Chen, L. Leng and H. Li, *Appl. Catal., B*, 2015, **174–175**, 445–454.
- 38 H. Wang, X. Yuan, Y. Wu, G. Zeng, X. Chen, L. Leng, Z. Wu, L. Jiang and H. Li, *J. Hazard. Mater.*, 2015, **286**, 187–194.
- 39 K. Mart  n-Betancor, S. Aguado, I. Rodea-Palomares, M. Tamayo-Belda, F. Legan  s, R. Rosal and F. Fern  ndez-Pi  as, *Sci. Total Environ.*, 2017, **595**, 547–555.
- 40 T. Thuy Duong, T. Son Le, T. H. T. Thi, T. Kien Nguyen, C. T. Ho, T. Hien Dao, P. Q. L. Thi, H. Chau Nguyen, D. K. Dang and T. H. L. Thi, *Adv. Nat. Sci.: Nanosci. Nanotechnol.*, 2016, **7**, 35018.
- 41 F. Mou, P. Wang, H. Li and Z. Zhou, *Journal of Convergence Information Technology*, 2013, **8**, 176–182.
- 42 X. Wang, X. Wang, J. Zhao, J. Song, J. Wang, R. Ma and J. Ma, *Chem. Eng. J.*, 2017, **320**, 253–263.



- 43 V. Aruoja, H. Dubourguier, K. Kasemets and A. Kahru, *Sci. Total Environ.*, 2009, **407**, 1461–1468.
- 44 C. C. Zhang, X. Y. Liu and Z. Y. Wang, *Appl. Mech. Mater.*, 2013, **328**, 758–762.
- 45 J. Ji, Z. Long and D. Lin, *Chem. Eng. J.*, 2011, **170**, 525–530.
- 46 D. Lin, J. Ji, Z. Long, K. Yang and F. Wu, *Water Res.*, 2012, **46**, 4477–4487.
- 47 L. Chen, L. Zhou, Y. Liu, S. Deng, H. Wu and G. Wang, *Ecotoxicol. Environ. Saf.*, 2012, **84**, 155–162.

